# MINLP optimization of a composite I beam floor system

Tomaž Žula [a], Stojan Kravanja [*] and Uroš Klanšek [b]

*University of Maribor, Faculty of Civil Engineering, Transportation Engineering and Architecture,*
*Smetanova 17, 2000 Maribor, Slovenia*

**Abstract.** This paper presents the cost optimization of a composite I beam floor system, designed to be made from a reinforced concrete slab and steel I sections. The optimization was performed by the mixed-integer non-linear programming (MINLP) approach. For this purpose, a number of different optimization models were developed that enable different design possibilities such as welded or standard steel I sections, plastic or elastic cross-section resistances, and different positions of the neutral axes. An accurate economic objective function of the self-manufacturing costs was developed and subjected to design, resistance and deflection (in)equality constraints. Dimensioning constraints were defined in accordance with Eurocode 4. The Modified Outer-Approximation/ Equality-Relaxation (OA/ER) algorithm was applied together with a two-phase MINLP strategy. A numerical example of the optimization of a composite I beam floor system, as presented at the end of this paper, demonstrates the applicability of the proposed approach. The optimal result includes the minimal produced costs of the structure, the optimal concrete and steel strengths, and dimensions.

**Keywords:** composite structures; cost optimization; structural optimization; mixed-integer non-linear programming; MINLP

## 1. Introduction

Composite concrete-steel floor systems represent cost-effective types of structures. The good technical and design characteristics of composite floors, particularly the compatible composition between two different materials with the concrete efficient in compression and the steel in tension have made their rational usages in building design exceedingly widespread. Consequently, the optimization of composite floors has developed into an attractive area of research and industrial application, frequently addressed nowadays in many published works.

The optimizations of composite structures can be, in general, performed under different criteria. However, as such building systems are built from different construction materials, the majority of researchers have focused on the cost optimizations of structures, where various cost parameters have been employed within the objective function rather than weights. In regard to specific types of composite structures, one can find a wide variety of different proposals in literature for the mathematical formulations of cost objective functions. As a result of significant progress regarding

---

[*]Corresponding author, Professor, Ph.D., E-mail: stojan.kravanja@um.si
[a] Assistant Professor, Ph.D., E-mail: tomaz.zula@um.si
[b] Associate Professor, Ph.D., E-mail: uros.klansek@um.si

computing and computer hardware, a number of different search techniques and efficient solution algorithms have been developed and successfully applied. For instance, Adeli and Kim (2001) proposed a neural dynamics approach for the optimizations of composite floors and developed a cost-objective function, which included the costs of concrete, steel beams, and shear studs. Kassapoglou and Dobyns (2001) simultaneously minimized the costs and weights of post-buckled stiffened composite panels using a gradient-based optimization method and created the Pareto set of optimum designs. Kravanja and Šilih (2003), as well as Klanšek and Kravanja (2006a, b), conducted research work in which the competition between different composite concrete-steel floor systems was investigated on the basis of cost optimization using non-linear programming. Also Klanšek *et al*. (2006) presented the cost optimization of composite floor trusses composed from steel trusses consisting of hot rolled channel sections, performed by the non-linear programming approach. Kovacs *et al*. (2004) optimized a carbon-fibre-reinforced plastic sandwich-like structure with aluminium webs using a multi-algorithm approach for minimum cost and maximum stiffness. During the optimization process they used the particle swarm optimization algorithm, a dynamic search technique, and a continuous-discrete optimization technique. Omkar *et al*. (2008, 2011) introduced a design optimization of composite structures based on an objective switching clonal selection algorithm and on a vector evaluated artificial bee colony algorithm. In the mentioned two works, the optimization problems included multiple objectives for minimizing weights and the total costs of composite components. Cheng and Chan (2009) calculated the optimal lateral stiffness designs of composite steel and concrete tall frameworks using an efficient numerical approach developed based on the optimality criteria method. The contribution of Senouci and Al-Ansari (2009) demonstrated the suitability of a genetic algorithm for the cost optimization of a composite structure under the load and resistance factor design. A cost-effective structural composition was introduced by Poitras *et al*. (2011), where the optimizations of composite and non-composite concrete-steel floor systems were performed using the particle swarm algorithm. Luo *et al*. (2012) developed a three-phase topology optimization model and an effective solution procedure for generating optimal material distributions for steel-concrete composite structures. The objective was to minimize the total material cost (or mass), whilst the optimal topology was obtained through a standard gradient-based search. For the purpose of obtaining the cost optimal design of a composite floor structure, Kaveh and Abadi (2010) utilised an improved harmony search algorithm, Kaveh and Behnam (2012) applied meta-heuristic algorithms: the charged system search and the enhanced charged system search, Kaveh and Ahangaran (2012) used a social harmony search, Kaveh and Massoudi (2012) introduced an ant colony algorithm, and Kaveh and Ghafari (2016) demonstrated the application of an enhanced colliding body optimization algorithm.

Finding an optimal discrete design of a concrete-steel composite structure still represents a challenging task because this optimization problem is discrete, non-convex, and highly non-linear. A state of the art literature review revealed that the discrete sizing and material optimizations of composite structures were mainly handled by different heuristic methods. The aim of this paper is to demonstrate discrete-continuous optimization, as performed by a mixed-integer non-linear programming (MINLP) approach. The treated composite floor system consisted of a reinforced concrete slab and doubly-symmetrical steel I beams. The optimization was proposed towards the direction of minimizing the structure's cost objective function, which was subjected to the design, resistance and deflection constraints as formulated in accordance with Eurocode standards (Eurocode 1 2002, Eurocode 2 2004, Eurocode 3 2005, Eurocode 4 2004) for satisfying the requirements of both the ultimate and serviceability limit states.

The MINLP is a combined discrete-continuous optimization method. It handles using continuous and discrete binary 0-1 variables simultaneously. The continuous variables are defined for the continuous optimization of parameters (costs, masses, dimensions, stresses, strains, etc.) and the discrete variables are used for the discrete optimization of standard/discrete sizes and materials (plate thicknesses, steel sections, the concrete and steel strengths). The MINLP performs the continuous and the discrete optimizations simultaneously through three steps: the first one includes the generation of a mechanical superstructure of different discrete alternatives, the second one involves the development of an MINLP model formulation and the last one consists of a solution for the defined MINLP optimization problem. The Modified Outer-Approximation/ Equality-Relaxation (OA/ER) algorithm is used for attaining the solution, see Kravanja and Grossmann (1994) and Kravanja *et al.* (1998a, b, c). Two-phase MINLP optimization is proposed to accelerate the convergence of the mentioned algorithm. The optimizations are carried out by an MINLP computer package MIPSYN (see Kravanja *et al.* (2003) and Kravanja (2010)).

This research represents a natural continuation of the past work presented by Kravanja *et al.* (2005), where the cost, material and standard dimension optimization was introduced for a composite floor system with welded steel I beams; the calculations based on the plastic cross-section resistance, the neutral and the centre of gravity axes lied in the concrete; a simple objective function was defined.

Standard steel sections are now explicitly used for the components of the composite floors. Two accurate cost objective functions of the material, power and labour costs are defined for those structures with welded and standard steel sections. Since there exist various different design possibilities, various optimization models are thus developed as the combination between: three different cross-section alternatives (with welded, HEA and IPE steel sections), two different composite cross-section resistances (the plastic and elastic resistances), three different positions of the composite cross-section's neutral axis (within the concrete slab, the upper steel flange and the steel web), and two different positions of the centre of gravity axis of the transformed (all-steel) section (within the concrete slab and the steel section). Rounding the depth of the concrete slab by a whole cm is also explicitly added into the optimization. Last but not least, sets of logical and design conditions are formulated with regard to the latest Eurocode 4 (2004).

## 2. Composite floor system

The structural system, represents a composite floor that consisted of a reinforced concrete slab and symmetrical steel I sections, see Fig. 1. The steel sections and the slab were connected together by headed shear studs, welded to the upper steel flanges and embedded within the concrete. A full shear connection between the concrete slab and the steel sections was considered.

From the resistance point of view, the composite floor system is considered as a multitude of equal composite I beams arranged in parallel at equal intermediate distances *e*, see Fig. 2. Each composite I beam is additionally composed of the effective part of the concrete slab $b_{eff}$ and a single steel section. The composite I beams are treated as simply supported beams. The concrete slab is considered as being designed separately as a continuous one way spanning slab of constant depth over the steel sections. It is assumed that a fresh concrete is placed to its final position by means of concrete pumps. A fully prefabricated formwork system is used in order to bear the wet concrete and steel I beams in the phase of concreting. The composite beams have to be designed according to Eurocode 4 (2004) standards. In addition, the reinforced concrete slab has to satisfy
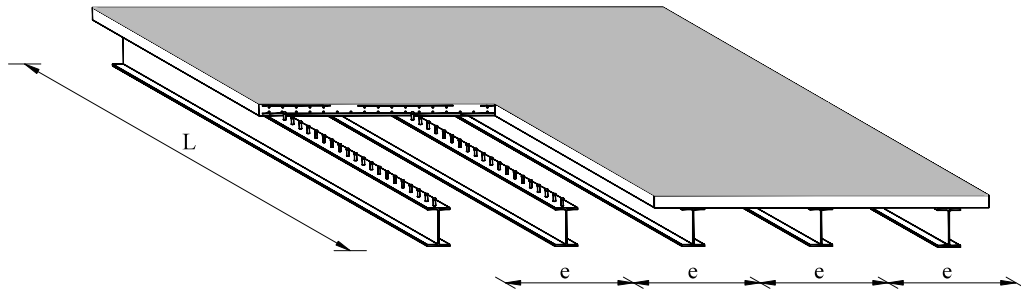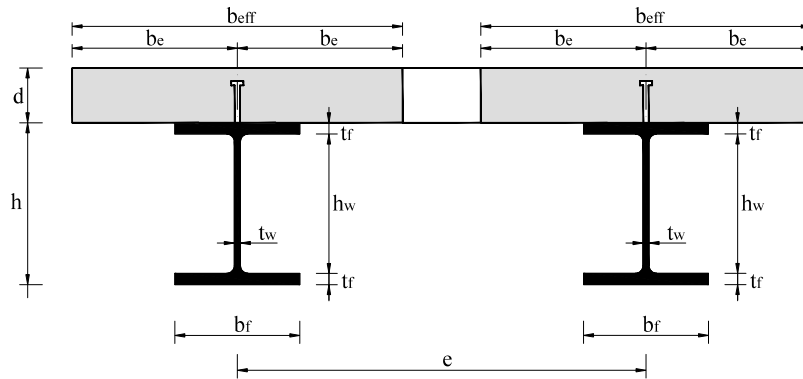
Fig. 1 Composite floor system



Fig. 2 Vertical cross-section of the composite floor system

the requirements of Eurocode 2 (2004), whilst the structural steel members should fulfil the conditions of Eurocode 3 (2005).

The structure should support the combined effect of its own weight and the uniformly distributed variable imposed load. As soon as the design load is set, the composite floor structure is checked for the conditions of both the ultimate and serviceability limit states. When the ultimate limit state has been addressed, the floor system should be checked for the resistance to the bending moment of the effective composite cross-section, for the shear resistance and shear buckling resistance of the steel section, the bearing/shear resistance of the headed shear stud connectors, and for resistance to the bending moment of the concrete slab. When the serviceability limit state has been considered, vertical deflections of the composite floor structure are checked by taking into account the second moment of the transformed (all-steel) cross-section area and the influence of creep/shrinkage of the concrete. The verification conditions are established for the total deflection of composite I beam due to the overall load, for the deflection caused by the variable imposed load, and for total deflection of the reinforced concrete slab which occurs due to the overall load over the span between the steel beams.

## 3. Optimization models COMBOPT

As the optimization problem of the composite floor system is discrete, non-convex and highly non-linear, the mixed-integer non-linear programming (MINLP) is selected for this application.

*3.1 General* MIN*LP problem formulation*

The non-convex, non-linear and combined discrete-continuous optimization problem can be formulated as a general MINLP problem in the following form

$$\min \quad z = \mathbf{c}^{\mathrm{T}}\mathbf{y} + f(\mathbf{x})$$

$$\text{s.t.} \quad \mathbf{h}(\mathbf{x}) = \mathbf{0}$$

$$\mathbf{g}(\mathbf{x}) \le \mathbf{0} \qquad \qquad \text{(MINLP)}$$

$$\mathbf{By} + \mathbf{Cx} \le \mathbf{b}$$

$$\mathbf{x} \in X = \{\mathbf{x} \in R^{n}: \quad \mathbf{x}\mathrm{LO} \le \mathbf{x} \le \mathbf{x}\mathrm{UP}\}$$

$$\mathbf{y} \in Y = \{0,1\}^{m}$$

where $\mathbf{x}$ is a vector of the continuous variables specified in the compact set $X$ and $\mathbf{y}$ is a vector of the discrete binary 0-1 variables. Functions $f(\mathbf{x})$, $\mathbf{h}(\mathbf{x})$ and $\mathbf{g}(\mathbf{x})$ are non-linear functions involved in the objective function $z$, the equality and inequality constraints, respectively. All functions $f(\mathbf{x})$, $\mathbf{h}(\mathbf{x})$ and $\mathbf{g}(\mathbf{x})$ have to be continuous and differentiable. The expression $\mathbf{By} + \mathbf{Cx} \le \mathbf{b}$ represents a subset of mixed linear equality/inequality constraints, which must be fulfilled for discrete decisions and structure configurations. The objective function $z$ contains fixed costs caused by discrete decisions in the term $\mathbf{c}^{\mathrm{T}}\mathbf{y}$ while the dimension dependant costs are included in the function $f(\mathbf{x})$.

Continuous variables including costs, masses, dimensions, cross-section characteristics, loadings, internal forces, deflections, etc., and binary 0-1 variables are used here for the choices of discrete/standard cross-sections and materials. Equality and inequality constraints and the bounds of the variables represent a rigorous system of the design, loading, resistance, deflection, etc. constraints known from structural analysis and dimensioning. The mixed linear equality/inequality constraints are used for defining the relationships between the binary variables and determining the standard sizes and discrete materials. The optimizations of the structures may include various objectives worth considering. This paper proposes an objective function for minimizing the structure's self-manufacturing costs.

*3.2 Optimization models*

According to the above general MINLP problem formulation, 36 different MINLP optimization models COMBOPT (COMposite Beam OPTimization) were developed for the optimizations of the composite I beams. They included different design possibilities, defined as the combinations between:

- 3 various composite cross-section alternatives, with:
  - welded steel I sections,
  - standard HEA sections,
  - standard IPE sections,
- 2 different composite cross-section resistances:
  - plastic resistance,
  - elastic resistance,

- 3 different positions of the composite cross-section's neutral axis, within:
  o  the concrete slab,
  o  the upper steel flange,
  o  the web of the steel section,
- 2 different positions of the centre of gravity axis of the transformed (all-steel) section, within:
  o  the concrete slab and
  o  the steel section.

As an interface for mathematical modelling and data inputs/outputs, GAMS (General Algebraic Modelling System), a high level language, was used (Brooke *et al*. 1988).

Each model contained input data, continuous variables, discrete variables, and the cost objective function which was subjected to structural analysis constraints, dimensioning constraints and logical constraints, see Fig. 3. The structural analysis and dimensioning constraints were comprised of ultimate limit state (ULS) constraints such as the plastic or elastic bending resistances of the composite cross-section, the shear resistance, the resistances of the connectors and the cross-section resistance of the concrete slab, as well as the serviceability limit state (SLS) constraints for checking the vertical deflections of the composite beam and the concrete slab. Whilst the ULS constraints were defined for three different positions of the cross-section's neutral axis, the SLS constraints were determined for two different positions of the centre of gravity axis regarding the transformed section. Whilst the paper presents the objective functions and their cost items for composite I beams with welded and standard steel sections, only the main input data, variables and the main constraints are shown in Table 1.

### 3.3 Cost objective functions

In this paper, two objective functions of self-manufacturing (direct) costs for the optimization of a composite floor system with welded sections, as well as for those with standard hot rolled sections, were developed on the basis of cost items, as proposed in our previous work, see Klanšek and Kravanja (2006a, b).

The direct costs were determined as a sum of the material costs, the power consumption costs and the labour costs necessary for the production. In this way, the objective function for cost optimization of the composite I beam with welded sections was defined in the following form:

$$
\begin{aligned}
\min: COST = \{ &C_{M,s} + C_{M,c} + C_{M,r} + C_{M,sc} + C_{M,e} + C_{M,ac,fp,tc} + C_{M,f} \\
&+ C_{M,c,ng} + C_{M,c,oxy} + C_{P,c,gm} + C_{P,w} + C_{P,sw} \\
&+ C_{P,v} + C_{L,c,oxy\text{-}ng} + C_{L,g} + C_{L,p,a,t} + C_{L,w} + C_{L,sw} \\
&+ C_{L,spp} + C_{L,f} + C_{L,r} + C_{L,c} + C_{L,v} + C_{L,cc} \} / (e \cdot L)
\end{aligned}
\tag{1}
$$

where *COST* represents the direct costs per m$^2$ of the useable surface of the structural system; *L* stands for the span of the composite beam and *e* denotes the intermediate distance between the steel I-sections. Notations $C_M,...,$ $C_P,...$ and $C_L,...,$ represent the material, power and labour cost items that were included in the objective function. Here, the material costs were comprised of: structural steel $C_{M,s}$, concrete $C_{M,c}$, reinforcement $C_{M,r}$, headed shear studs $C_{M,sc}$, electrode consumption $C_{M,e}$, anti-corrosion, fire protection and top coat painting $C_{M,ac,fp,tc}$, floor-slab panels $C_{M,f}$, natural gas consumption $C_{M,c,ng}$, and oxygen consumption $C_{M,c,oxy}$. Furthermore, the power

```
┌─────────────────────────────────────────────┐
│           OPTIMIZATION MODELS COMBOPT          │
│                                                │
│               Cost objective function          │
│                        s.t.                     │
│                                                │
│   Structural analysis and dimensioning constraints │
│          -Ultimate limit state constraints      │
│              -Plastic bending resistance or      │
│                Elastic bending resistance        │
│                   -Shear resistance              │
│                 -Resistance of connectors        │
│              -Resistance of the concrete slab    │
│        -Serviceability limit state constraints   │
│             -Deflection of the composite beam    │
│              -Deflection of the concrete slab    │
│                                                │
│               Logical constraints for           │
│                  -Discrete materials             │
│                 -Standard dimensions             │
│                 -Rounded dimensions              │
│                                                │
│           Variables x, y and input data         │
└─────────────────────────────────────────────┘
```
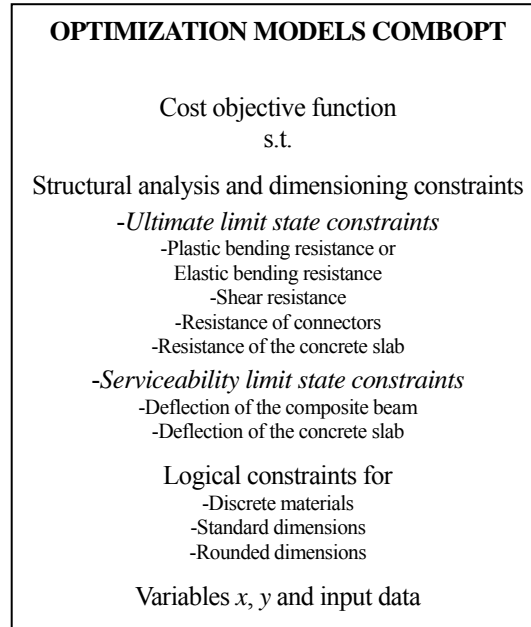
Fig. 3 Scheme of the optimization models COMBOPT

consumption cost contained: edge grinding $C_{P,c,gm}$, shielded metal arc welding $C_{P,w}$, stud arc welding $C_{P,sw}$ and concrete consolidation $C_{P,v}$. Finally, the labour costs consisted of: steel-sheet cutting $C_{L,c,oxy-ng}$, edge grinding $C_{L,g}$, preparation, assembly and tacking $C_{L,p,a,t}$, shielded metal arc welding $C_{L,w}$, stud arc welding $C_{L,sw}$, steel surface preparation and protection $C_{L,spp}$, formwork treatment $C_{L,f}$, reinforcing steel treatment $C_{L,r}$, concreting the slab $C_{L,c}$, concrete consolidation $C_{L,v}$ and curing the concrete $C_{L,cc}$. Note that detailed formulations for all the mentioned cost items can be found in Klanšek and Kravanja (2006a, b).

Compared to the above cost objective function for the composite structure with welded steel sections, the design with standard hot rolled sections needed a decreased amount of cost expressions to be covered, mainly due to the smaller amounts of welding processes and plate cuttings. More precisely, the contents of cost items $C_{M,e}$, $C_{M,c,ng}$, $C_{M,c,oxy}$, $C_{P,c,gm}$, $C_{P,w}$, $C_{L,c,oxy-ng}$, $C_{L,g}$ and $C_{L,w}$ were reduced on account of the absence of longitudinal welds and sheet metal cutting (except for vertical stiffeners), whilst the complete cost item $C_{L,p,a,t}$ was not incorporated for the same reason.

Although the above objective function presentation seems very similar to those presented in our previous work (Klanšek and Kravanja 2006a, b), there is an important new feature included within the objective. Namely, on the local markets, unit prices of structural steel sheets and sections often depend on their sizes and material grades. Regarding standard sizes, the thickness of a structural steel sheet and the height of standard I-section are typically those dimensions that have the greatest impact on the unit price $c_{M,s}$. Generally, thicker sheet thicknesses $t$, higher steel sections $h$ and stronger steel strengths $f_y$ show higher unit prices of steel $c_{M,s}$ than lower ones. The unit prices of structural steel sheets $c_{M,s} = f(t, f_y)$ and of standard I-sections $c_{M,s} = f(h, f_y)$ were thus included within the cost objective functions by applying approximation functions. The approximation functions were formulated by executing multiple regression using MS Excel software with Data

Table 1 Input data, continuous and discrete variables

| Input data: | | | |
|---|---|---|---|
| $b_{cu}$ | unit width of the concrete slab | $b_{eff}$ | effective width of the concrete slab |
| $c_L$ | labour prices per unit | $b_f$ | flange width |
| $c_P$ | power prices per unit | $COST$ | self-manufacturing costs of the structure per m$^2$ |
| $c_M$ | all the material prices per unit | $d$ | concrete slab depth |
| $d_{sc}$ | shear stud diameter | $e$ | the intermediate distance between the steel I-sections |
| $E_a$ | elastic modulus of structural steel | $E_{cm}$ | secant elastic modulus of normal weight concrete |
| $E_{c,eff}$ | effective elastic modulus of concrete | $f_{ck}$ | characteristic cylinder strength of concrete |
| $f_{ya}$ | yield strength of the reinforcing steel | $f_{ctm}$ | axial tensile strength of concrete |
| $f_u$ | ultimate tensile strength of the shear studs | $f_y$ | yield strength of structural steel |
| $L$ | structure span | $g$ | self-weight of the composite beam |
| $q$ | variable imposed load per m$^2$ | $h$ | height of the steel section |
| $q_m$ | discrete alternatives for standard materials (concrete and steel strengths) | $I_c$ | second moment of the unit cross-section area of a cracked concrete slab about the y-y axis |
| $q_r$ | discrete alternative values of rounded dimensions (depth of the concrete slab was proposed as being rounded up to a whole centimetre) | $I_{cr}$ | second moment of area of the transformed cross-section related to the creep of the concrete about the y-y axis |
| $q_s$ | discrete values of alternatives for standard dimensions (thicknesses of steel sheets for welded sections and sizes of IPE and HEA standard sections) | $I_i$ | second moment of area of the transformed cross-section about the y-y axis |
| $\alpha$ | coefficient related to the slenderness of the headed shear stud connector | $I_{sh}$ | second moment of area of the transformed cross-section regarding shrinkage of the concrete about the y-y axis |
| $\gamma_a$ | resistance partial safety factor for structural steel (1.0) | $I_u$ | second moment of the unit cross-section area of a non-cracked concrete slab about the y-y axis |
| $\gamma_c$ | resistance partial safety factor for concrete (1.5) | $n$ | modular ratio |
| $\gamma_g$ | partial safety factor for the permanent load (1.35) | $n_{sc}$ | number of headed shear studs |
| $\gamma_s$ | partial safety factor for the reinforcing steel (1.15) | $t_f$ | flange thickness |
| $\gamma_{MI}$ | partial safety factor for element instability (1.0) | $t_w$ | web thickness |
| $\gamma_v$ | resistance partial safety factors for the headed shear studs (1.25) | $x_p, x_e$ | vertical position of the plastic and elastic neutral axes of the composite beam from the top edge |
| $\gamma_q$ | partial safety factor for variable load (1.5) | $x_{pc}$ | vertical position of the plastic neutral axis of the concrete slab from the top edge |
| $\rho_c$ | density of concrete | $x_g$ | vertical position of the centre of gravity axis of the transformed (all-steel) section from the top edge |
| $\rho_s$ | density of steel | $\chi_v$ | shear buckling factor |
| *Continuous variables* $\mathbf{x} \in X$: | | *Discrete binary variables* $\mathbf{y} = \{\mathbf{y}^{mat}, \mathbf{y}^{st}, \mathbf{y}^{rd}\}$, $\mathbf{y} \in Y$: | |
| $A_a$ | cross-section area of the steel beam | $\mathbf{y}^{mat}$ | the sub-vector of the binary variables for standard materials |
| $A_s$ | cross-section area of the concrete slab reinforcement per m | $\mathbf{y}^{st}$ | the sub-vector for standard dimensions |
| $b_e$ | half of the effective width of the concrete slab | $\mathbf{y}^{rd}$ | the sub-vector for rounded dimensions |

Analysis Add-in. Bivariate quadratic functions, i.e., functions of a form $K(x, y) = a_1 x^2 + a_2 y^2 + a_3 xy + a_4 x + a_5 y + a_6$, were employed to achieve suitable approximations and to keep the non-convexities of the optimization models as low as possible. In this way, the unit prices for structural steel sheets and standard steel sections were gained by expressions $c_{M,s}$, see Eqs. (1a)-(1c)

Structural steel sheets: $\qquad c_{M,s} = c_s\,(a_1\,f_y^2 + a_2\,t^2 + a_3\,f_y\,t + a_4\,f_y + a_5\,t + a_6)$ (1a)

Structural steel I-sections: $\qquad c_{M,s} = c_s\,(a_1\,f_y^2 + a_2\,h^2 + a_3\,f_y\,h + a_4\,f_y + a_5\,h + a_6)$ (1b)

Concrete: $\qquad c_{M,c} = c_c\,(a_1\,f_{ck}^2 + a_2\,f_{ck} + a_3)$ (1c)

*Notes: Material grades $f_y$ and $f_{ck}$ are defined in [kN/cm$^2$], whilst dimensions $h$ and $t$ in [cm].*

The coefficients of the approximation functions for steel sheets, IPE and HEA sections are presented in Table 2, which also includes a function of the unit price for concrete. Whilst $a_1$, $a_2$,.., $a_6$ represent the coefficients of the approximation functions, $c_s$ denotes the basic unit price of the

Table 2 Unit prices for structural steel and concrete

| Material | Basic unit price | Coefficients of approximation function for unit price | | | | | |
|---|---|---|---|---|---|---|---|
| | | $a_1$ | $a_2$ | $a_3$ | $a_4$ | $a_5$ | $a_6$ |
| Steel sheet | $c_s = 1.25$ €/kg | $-3.7313 \times 10^{-4}$ | $-1.7170 \times 10^{-2}$ | $-4.9858 \times 10^{-4}$ | $2.8962 \times 10^{-2}$ | $1.2934 \times 10^{-1}$ | $4.4147 \times 10^{-1}$ |
| IPE section | $c_s = 1.25$ €/kg | $1.8783 \times 10^{-4}$ | $3.0707 \times 10^{-4}$ | $1.6530 \times 10^{-5}$ | $-3.3288 \times 10^{-3}$ | $-1.3915 \times 10^{-2}$ | $1.0630 \times 10^{0}$ |
| HEA section | $c_s = 1.25$ €/kg | $2.1982 \times 10^{-4}$ | $6.2266 \times 10^{-5}$ | $4.1031 \times 10^{-5}$ | $-5.3682 \times 10^{-3}$ | $4.9888 \times 10^{-4}$ | $9.8361 \times 10^{-1}$ |
| Concrete | $c_c = 85.00$ €/m$^3$ | $-3.2220 \times 10^{-2}$ | $4.0571 \times 10^{-1}$ | $1.8829 \times 10^{-1}$ | – | – | – |

Notes: Basic unit prices $c_s$ are set for the standard 8 mm thick steel sheet, standard IPE 80 and HEA 100 sections, all made from steel S 235. The unit price $c_c$ is defined for concrete C 25/30.
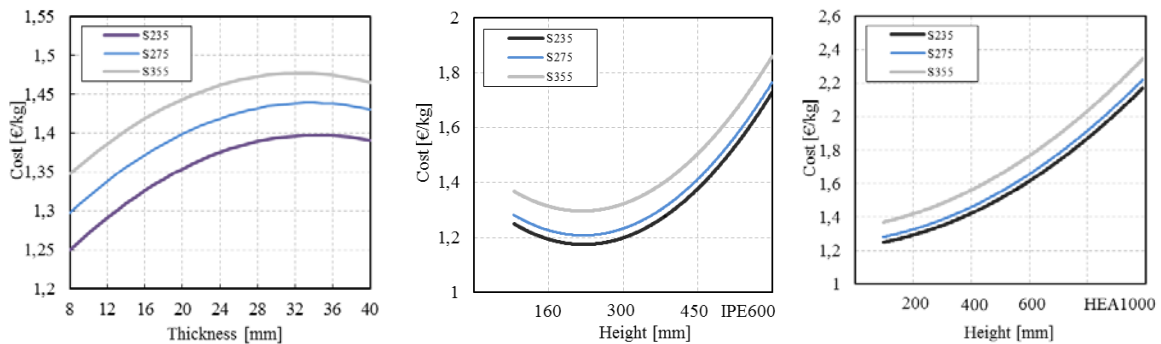


Fig. 4 Diagrammes of the unit prices for structural steel depending on the sheet thickness $t$ and the height of the IPE and HEA sections $h$

Table 3 Other material, power and labour cost parameters

| | | | |
|---|---|---|---|
| $c_{M,r}$ | Price of the steel-wire mesh reinforcement S 400 | 0.70 | €/kg |
| $c_{M,sc}$ | Price of the headed shear stud connectors | 0.50 | €/stud |
| $c_{M,e}$ | Price of the electrodes | 1.70 | €/kg |
| $c_{M,ac}$ | Price of the anti-corrosion paint | 0.85 | €/m² |
| $c_{M,fp}$ | Price of the fire protection paint R 30 | 9.00 | €/m² |
| $c_{M,tc}$ | Price of the top coat paint | 0.65 | €/m² |
| $c_{M,f}$ | Price of the prefabricated floor-slab panels | 30.00 | €/m² |
| $c_{M,ng}$ | Price of the natural gas | 0.50 | €/m³ |
| $c_{M,oxy}$ | Price of the oxygen | 1.60 | €/m³ |
| $c_P$ | Electric power price | 0.10 | €/kWh |
| $c_L$ | Labour costs | 20.00 | €/h |

steel sheet/I-section with the lowest standard thickness/height and steel grade. A coefficient $c_c$ stands for the basic unit price of the concrete with the lowest concrete strength. Fig. 4 shows diagrammes of the unit prices for structural steel depending on the sheet thickness $t$ and the IPE and HEA section heights $h$ for three different structural steel grades: S 235, S 275 and S 355. Other material unit prices and hourly labour costs are shown in Table 3.

### 3.4 Structural analysis and dimensioning constraints

In order to achieve optimal design of the composite floor structure, the objective functions should be subjected to various design conditions. Here, (in)equality constraints and the bounds on decision variables represent a rigorous system of design, load, resistance and deflection functions in order to satisfy the requirements of Eurocode 4 for the conditions of the ultimate and serviceability limit states, see Eqs. (2)-(20), Eqs. (21)-(37) and Appendixes A and B, respectively. As many of these functions are well-known from Eurocode and literature, they are presented in this paper in brief forms. For better understanding please see the input data - scalars and the variables in Section 3.2.

### 3.5 Ultimate limit state constraints

#### 3.5.1 Plastic bending resistance of the composite beam cross-section

Eqs. (2)-(4) represent the basic condition for the plastic moment resistance of the composite I beam cross-section. Whilst $M_{Ed,cb}$ stands for the design bending moment, $M_{pl,Rd,cb}$ denotes the design plastic moment resistance of the composite section. Equations $M_{pl,Rd,cb}$ are shown in Appendix A. The design uniformly distributed load on the composite beam $q_{Ed,cb}$ is calculated by Eq. (4). Whilst the variable imposed load $q$ is determined as an input constant, the dead-weight of the structure $g$ is automatically calculated through the optimization process depending on the obtained composite cross-section area's dimensions.

$$M_{Ed,cb} \leq M_{pl,Rd,cb} \tag{2}$$

where

$$M_{Ed,cb} = q_{Ed,cb} \cdot L^2 / 8 \qquad (3)$$

$$q_{Ed,cb} = \left( \gamma_g \cdot g + \gamma_q \cdot q \cdot e \right) \qquad (4)$$

### 3.5.2 Elastic bending resistance of the composite beam cross-section

In the case when the elastic resistance of the composite structure is considered, the basic condition for the elastic moment resistance of the composite cross-section is given by Eq. (5). The design bending moment $M_{Ed,cb}$ is defined by Eq. (3), whilst the design elastic bending moment resistance $M_{el,Rd,cb}$ is presented in Appendix B.

$$M_{Ed,cb} \leq M_{el,Rd,cb} \qquad (5)$$

### 3.5.3 Shear resistance of the composite beam cross-section

Shear resistance is here assured by the shear resistance of the web of the steel section. Eqs. (6)-(8) introduce the condition for the shear resistance, where $V_{Ed,cb}$ in Eq. (7) represents the design shear force and $V_{b,Rd,cb}$ shown in Eq. (8) denotes the shear buckling resistance of the steel web. Note that at the end of the beams, the web stiffeners are added to prevent local buckling of the web.

$$V_{Ed,cb} \leq V_{b,Rd,cb} \qquad (6)$$

where

$$V_{Ed,cb} = \frac{q_{Ed,cb} \cdot L}{2} \qquad (7)$$

$$V_{b,Rd,cb} = \frac{\chi_v \cdot f_y \cdot \left( h - 2 \cdot t_f \right) \cdot t_w}{\sqrt{3} \cdot \gamma_{M1}} \qquad (8)$$

### 3.5.4 Resistance of shear connectors

The proper transfer of the design longitudinal shear force $V_l$ between the concrete slab and the steel section is ensured using a sufficient number of welded stud connectors $n_{sc}$ and the design resistances of the connectors $P_{Rd}$, see Eqs. (9)-(11).

$$V_l = 1/2 \cdot n_{sc} \cdot P_{Rd} \qquad (9)$$

where

$$V_l = \min \left\{ \frac{A_a \cdot f_y}{\gamma_a} ; \frac{2 \cdot b_e \cdot d \cdot 0.85 \cdot f_{ck}}{\gamma_c} \right\} \qquad (10)$$

$$P_{Rd} = \min \left\{ \frac{0.29 \cdot \alpha \cdot d_{sc}^2 \cdot \sqrt{f_{ck} \cdot E_{cm}}}{\gamma_v} ; \frac{0.8 \cdot f_u \cdot \pi \cdot d_{sc}^2}{4 \cdot \gamma_v} \right\} \qquad (11)$$

### 3.5.5 Resistance of the concrete slab

The condition for the bending moment resistance of the concrete slab is introduced by Eqs. (12)-(15). For both the plastic or elastic design cases, the plastic and the elastic design bending moments $M_{Ed,cs,pl}$ and $M_{Ed,cs,el}$, are defined by Eqs. (13) and (14), whilst the design uniformly

distributed load on the concrete slab $q_{Ed,cs}$ is calculated by Eq (15). The design ultimate moment capacity of the concrete slab $M_{ult,cs}$ is given by Eq. (16). The area of reinforcing steel is calculated by Eqs. (17)-(20). The requirements for the minimum area of reinforcing steel $A_{s,\min}$ and the maximum area of reinforcing steel $A_{s,\max}$ are handled by the constraints in Eqs. (17)-(20), where $k_c$ is the coefficient which takes account of the stress distribution within the section immediately prior to cracking and of the change of the lever arm and $k_l$ is the coefficient which allows for the effect of non-uniform self-equilibrating stresses, which lead to a reduction of restraint forces.

$$M_{Ed,cs} \leq M_{ult,cs} \tag{12}$$

where

$$M_{Ed,cs,pl} = q_{Ed,cs} \cdot e^2 / 16 \tag{13}$$

$$M_{Ed,cs,el} = q_{Ed,cs} \cdot e^2 / 11.67 \tag{14}$$

$$q_{Ed,cs} = \left( \gamma_g \cdot \rho_c \cdot b_{cu} \cdot d + \gamma_q \cdot q \cdot b_{cu} \right) \tag{15}$$

$$M_{ult,cs} = \frac{0.48 \cdot 0.85 \cdot f_{ck} \cdot b_{cu} \cdot x_{pc}^2}{\gamma_c} + \frac{A_s \cdot b_{cu} \cdot (d - c - x_{pc}) \cdot f_{ya}}{\gamma_s} \tag{16}$$

$$A_{s,\min} \cdot \sigma_s = k_c \cdot k_l \cdot f_{ct,eff} \cdot A_{ct} \tag{17}$$

$$A_{s,\min} \geq 0.26 \cdot f_{ctm} / f_{yk} \cdot b_{cu} \cdot (d - c) \tag{18}$$

$$A_{s,\min} \geq 0.0013 \cdot b_{cu} \cdot (d - c) \tag{19}$$

$$A_{s,\max} \leq 0.04 \cdot b_{cu} \cdot d \tag{20}$$

### 3.6 Serviceability limit state constraints

#### 3.6.1 Vertical deflection of the composite beam

The serviceability limit state constraints comprise Eqs. (21)-(37). The vertical deflections of the composite I beam are checked by the conditions handled in Eqs. (21)-(26), where $\delta_2$ is the deflection of the composite I beam subjected to a variable imposed load, $\delta_{\max}$ is the deflection of the composite I beam subjected to the overall load, $\delta_{cr}$ is the deflection of the composite I beam subjected to a permanent load and a creep of concrete, $\delta_{sh}$ is the deflection of the composite I beam subjected to shrinkage of concrete and $M_{sh}$ is the bending moment caused by the shrinkage of concrete.

$$\delta_2 \leq L/300 \tag{21}$$

$$\delta_2 = \frac{5 \cdot q \cdot e \cdot L^4}{384 \cdot E_a \cdot I_i} \tag{22}$$

$$\delta_{\max} \leq L/250 \tag{23}$$

$$\delta_{\max} = \delta_2 + \delta_{cr} + \delta_{sh} \tag{24}$$

$$\delta_{cr} = \frac{5 \cdot g \cdot L^4}{384 \cdot E_a \cdot I_{cr}} \tag{25}$$

$$\delta_{sh} = \frac{M_{sh} \cdot L^2}{8 \cdot E_a \cdot I_{sh}} \tag{26}$$

As mentioned, two different possibilities exist for the positions of the centre of gravity axis of the transformed (all-steel) section $A_i$: namely within the concrete slab or within the steel section. When the centre of gravity axis lies within the concrete slab, see Fig. 5, the vertical distance $x_g$ from the top of the concrete slab to the centre of gravity axis is defined by Eqs. (27)-(28) and the second moment of area regarding the transformed section $I_i$ is determined by Eq. (29).

$$x_g \leq d \tag{27}$$
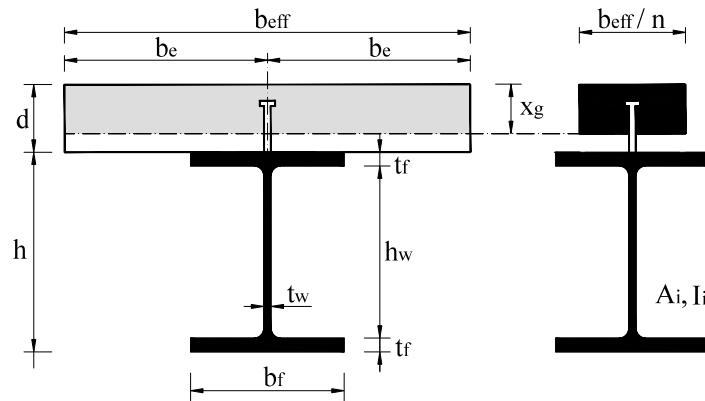


Fig. 5 Centre of gravity axis situated within the concrete slab
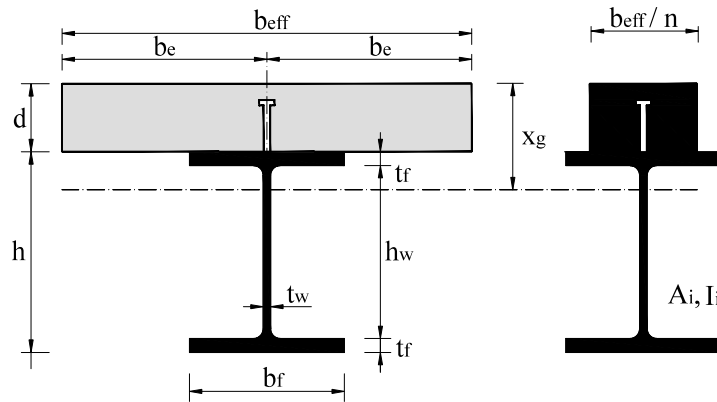


Fig. 6 Centre of gravity axis situated within the steel section

$$x_g = \frac{-A_a + \sqrt{A_a^2 + 2 \cdot \frac{b_{eff}}{n} \cdot A_a \cdot \left(d + \frac{h}{2}\right)}}{\frac{b_{eff}}{n}} \tag{28}$$

$$I_i = \frac{b_{eff} \cdot x_g^3}{3 \cdot n} + I_a + A_a \cdot \left(d + \frac{h}{2} - x_g\right)^2 \tag{29}$$

Eqs. (30)-(32) represent the constraints for the centre of gravity axis of the transformed section $x_g$ positioned within the steel section, see Fig. 6. The moment of inertia of the transformed section $I_i$ is calculated by Eq. (32).

$$x_g \geq d \tag{30}$$

$$x_g = \frac{\frac{b_{eff} \cdot d^2}{2 \cdot n} + A_a \cdot \left(d + \frac{h}{2}\right)}{\frac{b_{eff} \cdot d}{n} + A_a} \tag{31}$$

$$I_i = \frac{b_{eff}}{n} \cdot \left[\frac{d^3}{12} + d \cdot \left(x_g - \frac{d}{2}\right)^2\right] + I_a + A_a \cdot \left(d + \frac{h}{2} - x_g\right)^2 \tag{32}$$

### 3.6.2 Vertical deflection of the concrete slab

The condition for vertical deflections of the concrete slab is defined by Eqs. (33)-(37), where $\delta$ represents the total deflection of the reinforced concrete slab subjected to the overall load, $\delta_I$ stands for the deflection of a non-cracked reinforced concrete slab subjected to the overall load and $\delta_{II}$ denotes the deflection of a cracked reinforced concrete slab subjected to the overall load. Whilst $\zeta$ is the distribution coefficient, $\sigma_{sr}$ is the stress in tension steel reinforcement calculated on the basis of a cracked concrete section under the loading which will just cause cracking, and $k$ defines the coefficient which depends on the number of spans of the continuous concrete slab.

$$\delta \leq L/250 \tag{33}$$

$$\delta = \zeta \cdot \delta_{II} + (1 - \zeta) \cdot \delta_I \tag{34}$$

$$\zeta = 1 - 0.5 \cdot \sigma_{sr}/\sigma_s \tag{35}$$

$$\delta_I = k \cdot \left(\frac{\rho_c \cdot b_{cu} \cdot d \cdot e^4}{E_{c,eff} \cdot I_u} + \frac{q \cdot b_{cu} \cdot e^4}{E_{cm} \cdot I_u}\right) \tag{36}$$

$$\delta_{II} = k \cdot \left(\frac{\rho_c \cdot b_{cu} \cdot d \cdot e^4}{E_{c,eff} \cdot I_c} + \frac{q \cdot b_{cu} \cdot e^4}{E_{cm} \cdot I_c}\right) \tag{37}$$

### 3.7 Logical constraints

Logical constraints define discrete values for standard materials $d^{mat}$, standard dimensions $d^{st}$

and rounded dimensions $d^{rd}$, see Eqs. (38)-(43). The standard material $d^{mat}$ (steel or concrete strength) is determined as a scalar product between the vector of $m$, $m \in M$, discrete standard strength alternatives $\mathbf{q}_m = \{q_1, q_2, q_3, \ldots, q_m\}$ and the vector of $m$ associated binary variables $\mathbf{y}_m^{mat} = \{y_1^{mat}, y_2^{mat}, y_3^{mat}, \ldots, y_m^{mat}\}$, see Eq. (38). Only one discrete strength value is selected for the material as the sum of the binary variables $y_m^{mat}$ has to be equal to 1, see Eq. (39).

$$d^{mat} = \sum_{m \in M} q_m y_m^{mat} \qquad m \in M \tag{38}$$

$$\sum_{m \in M} y_m^{mat} = 1 \qquad m \in M \tag{39}$$

The standard dimension $d^{st}$ (e.g., thickness of the steel sheet for the welded section, the cross-section area of IPE or HEA standard section, steel wire mesh for concrete, etc.) is defined as a scalar product between the vector of $s$, $s \in S$, discrete standard dimension alternatives $\mathbf{q}_s = \{q_1, q_2, q_3, \ldots, q_s\}$ and the vector of $s$ associated binary variables $\mathbf{y}_s^{st} = \{y_1^{st}, y_2^{st}, y_3^{st}, \ldots, y_s^{st}\}$, see Eq. (40). Only one discrete value is selected to the standard dimension as the sum of the binary variables $y_s^{st}$ has to be equal to 1, see Eq. (41).

$$d^{st} = \sum_{s \in S} q_s y_s^{st} \qquad s \in S \tag{40}$$

$$\sum_{s \in S} y_s^{st} = 1 \qquad s \in S \tag{41}$$

Similarly, the rounded dimension $d^{rd}$ (depth of the concrete slab is rounded to a whole cm) is calculated as a scalar product between the vector of $r$, $r \in R$, discrete rounded dimension alternatives $\mathbf{q}_r = \{q_1, q_2, q_3, \ldots, q_r\}$ and the vector of $r$ associated binary variables $\mathbf{y}_r^{rd} = \{y_1^{rd}, y_2^{rd}, y_3^{rd}, \ldots, y_r^{rd}\}$, see Eq. (42). Only one discrete value is selected as the rounded dimension (to the depth of the concrete slab) as the sum of the binary variables $y_r^{rd}$ has to be equal to 1, see Eq. (43).

$$d^{rd} = \sum_{r \in R} q_r y_r^{rd} \qquad r \in R \tag{42}$$

$$\sum_{r \in R} y_r^{rd} = 1 \qquad r \in R \tag{43}$$

## 4. MINLP solution

The Modified Outer-Approximation/Equality-Relaxation (OA/ER) algorithm by Kravanja and Grossmann (1994) was applied to execute the discrete optimization of the composite floor structure. The OA/ER optimization algorithm solves an alternative sequence of non-linear programming (NLP) sub-problems and mixed-integer linear programming (MILP) master problems, see Fig. 7. The NLP sub-problem corresponds to the continuous optimization of parameters for a composite structure with fixed materials and standard dimensions (with fixed 0-1 variables, calculated in the previous MILP), and yields an upper bound to the MINLP objective to
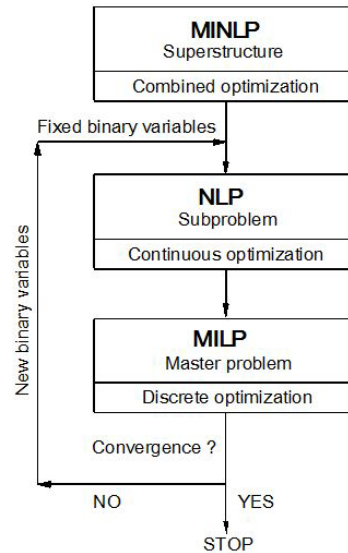
Fig. 7 The considered composite floor system

be minimized. The MILP master problem involves a global linear approximation to the superstructure of discrete alternatives in which new materials and standard sizes (new 0-1 variables) are identified. The predicted lower bounds increase monotonically as the cycle of the major MINLP iterations (MILP plus NLP) proceeds. A global linear approximation includes the linearizations of the non-linear objective function, the linearizations of the non-linear equality and inequality constraints, derived at each NLP sub-problem solution, as well as the linear constraints from the original MINLP problem. NLP sub-problems and MILP master problems must sequentially be solved until the convergence is satisfied. The search is completed when the predicted lower bound (MILP) coincides with or exceeds the current upper bound (NLP). In cases of non-convex problems, the optimization process is terminated when the NLP solution can no longer be improved. The main feature of the OA/ER algorithm is that the convergence is usually achieved in a few MINLP iterations (from three to seven). Subsequently, each MINLP iteration provides increasingly better result. More details about the Modified OA/ER algorithm can be found in Kravanja *et al*. (1998a, b, c).

The exact optimal solution of a complex, non-convex and non-linear MINLP problem with a high number of discrete decisions is, in general, very difficult to obtain. In this way, the MINLP optimization is proposed for being accomplished sequentially over two phases to accelerate the convergence of the Modified OA/ER algorithm, see also Kravanja *et al*. (2005):

- The search for optimal solution is proposed by starting with continuous NLP optimization of the composite superstructure, where all design parameters are treated as continuous variables. During the first phase, all discrete materials, standard and rounded dimensions are thus relaxed within continuous parameters. The result obtained at the end of the phase represents a good starting point for the next discrete optimization.
- When the optimal result of the continuous optimization is found, the search proceeds with the discrete optimization in the second phase. The discrete materials, standard and rounded sizes are re-established and the overall cost, material, standard and rounded dimension

optimization of the composite floor system will continue until the optimal solution is achieved.

The two-phase MINLP strategy requires that the binary variables should be defined in one uniform set and do not need to be initialized. Whilst the binary variables of the discrete alternatives and logical constraints for discrete decisions are in the first phase temporarily excluded from the optimization (set at zero value), they are at the beginning of the second phase included and participate in the simultaneous overall optimization. The data and variables are initialized only once at the beginning of the optimization. Under the convexity condition, the two-phase strategy guarantees a global optimality of the solution.

## 5. Numerical example – the simultaneous cost, material, standard and rounded dimension optimization

The numerical example presents the simultaneous cost, material, standard and rounded dimension optimization of a simply supported composite floor system with a span of 20 m, exposed to the combined effect of permanent uniform load (self-weight) and a uniformly distributed imposed load of 4 kN/m$^2$, see Fig. 8. The considered composite floor system is built up from the reinforced concrete slab and steel I sections. Individual steel beams and the concrete slab are connected together by the headed shear studs. The base diameter of the studs is 19 mm.

As there existed a number of different design possibilities for the composite floor structure, the MINLP optimization was performed 36 times for 36 different optimization models COMBOPT. This paper presents optimizations for plastic and elastic composite cross-section resistances for welded, standard HEA and IPE steel sections with three different positions of neutral axis: (a) within the concrete slab; (b) within the upper steel flange; and (c) within the steel web. Presented are only the results achieved in the case when the centre of gravity axis of the transformed section was positioned within the concrete slab because the results obtained in the case when the axis was situated in the steel section are worse.

The task of the optimization was to find the minimum material and labour costs of the structure, the optimal concrete and steel strengths, standard sizes of the steel beams, the distance between the beams and the depth of the concrete slab. The latter should be rounded to a whole cm.

### 5.1 Plastic cross-section resistance

In the case of the welded steel section, a superstructure was generated in which all possible structures were embedded within a combination between:
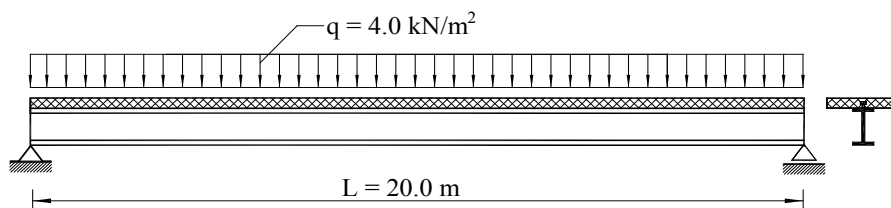


Fig. 8 The considered composite floor system

- 3 different ($m_{fy}$) structural steel grades (S 235, S 275, S 355), $m_{fy} \in M_{fy}$, $M_{fy} = \{1, 2, 3\}$;
- 7 different ($m_{ck}$) concrete strengths (C20/25, C25/30, C30/37, C35/45, C40/50, C45/55, C50/60), $m_{ck} \in M_{ck}$, $M_{ck} = \{1, 2, 3,..., 7\}$;
- 9 different ($s_{tf}$) standard steel thickness alternatives for flanges (from 8 to 40 mm), $s_{tf} \in S_{tf}$, $S_{tf} = \{1, 2, 3,..., 9\}$;
- 9 different ($s_{tw}$) standard steel thickness alternatives for webs (from 8 to 40 mm), $s_{tw} \in S_{tw}$, $S_{tw} = \{1, 2, 3,..., 9\}$;
- 25 different ($s_{mesh}$) discrete alternatives of steel wire meshes for reinforcing the concrete (from R188 to 5xR524), $s_{mesh} \in S_{mesh}$, $S_{mesh} = \{1, 2, 3,..., 25\}$ and
- 27 various ($r_d$) discrete alternatives for rounding up the depth of the concrete slab to a whole cm (from 4 to 30 cm), $r_d \in R_d$, $R_d = \{1, 2, 3,..., 27\}$.

In this way, the number of defined discrete binary variables was $m_{fy} + m_{ck} + s_{tf} + s_{tw} + s_{mesh} + r_d$ = 3 + 7 + 9 + 9 + 25 + 27 = 80, whilst the superstructure of alternatives was comprised of $m_{fy} \cdot m_{ck} \cdot s_{tf} \cdot s_{tw} \cdot s_{mesh} \cdot r_d = 3 \cdot 7 \cdot 9 \cdot 9 \cdot 25 \cdot 27 = 1.1481 \cdot 10^6$ various solutions of discrete variables.

The MINLP optimization model COMBOPT of the structure with welded steel I sections was used. The model included accurate cost objective function of the self-manufacturing material, power and labour costs, see Eq. (1). The optimization was carried out by the MINLP computer package MIPSYN, see Kravanja *et al.* (2003) and Kravanja (2010), the successor of PROSYN Kravanja and Grossmann (1994). The Modified OA/ER algorithm and the two-phased optimization were applied, where GAMS/CONOPT (generalised reduced-gradient method) by Drudd (1994) was used to solve NLP sub-problems, whilst GAMS/CPLEX (branch and bound method) was employed to find solutions to MILP master problems.

The generalized reduced gradient method (GRG), developed by Abadie and Carpentier (1969), is a generalization of the reduced gradient method (RG) by allowing non-linear constraints and arbitrary bound on the variables. The RG method, introduced by Wolfe (1976), solves the non-linear programming formulated problems and uses the equality constraints to eliminate a subset of the variables. The method reduces the original problem to a bound-constrained problem in the space of the remaining variables. The gradient methods handle with the search directions defined by the gradient of the function at the current point.

CPLEX applies well-known principles of the branch and bound method (BB), proposed by Land and Doig (1960), in order to solve mixed-integer linear programming (MILP) master problems. The BB is an efficient enumeration procedure for examining all possible integer feasible solutions. It manages a search tree consisting of nodes. Every node represents a sub-problem to be processed: i.e., to be solved, to be checked for integrality and perhaps to be further analyzed. The BB algorithm continues to select nodes for branching in the search tree until it finds all final nodes at the end of branches and the optimal integer solution.

The best result of the structure with welded steel sections was reached in the case when the neutral axis lay within the concrete slab, see the Welded case (a) in Table 4. The procedure began with continuous cost optimization of the relaxed material, standard and rounded dimensions. As all the variables were defined during this phase as being continuous, binary variables and their logical constraints were temporarily excluded from the optimization. An optimal cost of 79.19 € per m² of the structure was obtained using the continuous steel and concrete strengths and dimensions (the 1st NLP, Table 4). When the optimal result was reached, the procedure was resumed with the simultaneous cost, discrete material, standard and rounded dimension optimization at the second level. Binary variables and logical constraints for discrete decisions were added in the optimization

during this phase. The optimal result of 79.55 € per m² of the composite floor system was obtained during the 6th MINLP iteration (the 6th NLP, Welded case (a), Table 4). Alongside the optimal structure costs, the solution also comprised steel and concrete grades S 355 and C20/25, respectively, all dimensions of welded steel sections and their intermediate distances, depth of the concrete slab 18 cm and the reinforcement R257, see Fig. 9.

Table 4 Convergence of the Modified OA/ER algorithm for plastic resistance of the composite structure with welded, IPE and HEA sections; results - structure cost [€/m²]

| | Welded | | | IPE | | | HEA | | |
|---|---|---|---|---|---|---|---|---|---|
| | (a) | (b) | (c) | (a) | (b) | (c) | (a) | (b) | (c) |
| | Continuous optimization | | | | | | | | |
| 1. NLP | 79.19 | 87.08 | 100.86 | 194.05 | 179.71 | 176.67 | 128.27 | 140.61 | 172.61 |
| | Discrete material, standard and rounded dimension optimization | | | | | | | | |
| 1. MILP | 79.20 | 87.13 | 101.05 | 197.13 | 184.10 | 179.58 | 130.09 | 145.01 | 178.31 |
| 2. NLP | 82.09 | 87.13[*] | 101.05[*] | **197.20** | **184.10** | 179.68[*] | 130.51 | 148.90 | **179.40** |
| 2. MILP | 80.10 | 87.28 | 101.33 | 198.67 | 185.20 | 180.23 | 130.23 | 146.39 | 181.36 |
| 3. NLP | 80.24 | 87.28[*] | 101.33[*] | 198.62 | *184.79* | **180.20** | **130.26** | **148.37** | 180.84 |
| 3. MILP | 80.54 | 87.33 | 101.56 | - | - | 180.65 | 130.53 | 148.64 | - |
| 4. NLP | 79.81 | 87.33[*] | 101.56[*] | - | - | 181.52 | 130.68 | 150.07 | - |
| 4. MILP | 80.67 | 87.43 | 101.78 | - | - | - | - | - | - |
| 5. NLP | 79.74 | **87.89** | 101.78[*] | - | - | - | - | - | - |
| 5. MILP | 80.72 | 87.89 | 101.97 | - | - | - | - | - | - |
| 6. NLP | **79.55** | 88.49 | 101.97[*] | - | - | - | - | - | - |
| 6. MILP | 80.76 | - | 102.10 | - | - | - | - | - | - |
| 7. NLP | 80.11 | - | **102.44** | - | - | - | - | - | - |
| 7. MILP | - | - | 102.47 | - | - | - | - | - | - |
| 8. NLP | - | - | 102.80 | - | - | - | - | - | - |

The neutral axis lies within: (a) concrete slab; (b) upper steel flange; (c) steel web
[*] Locally infeasible solution (when a/some constraint(s) is/are not satisfied)
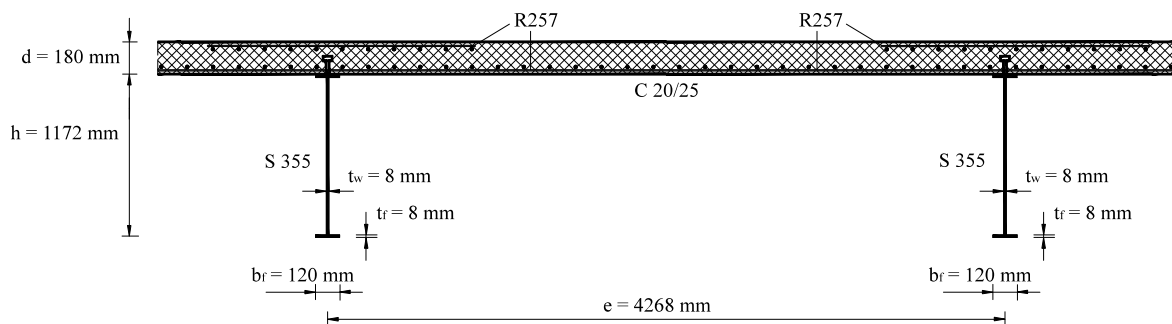


Fig. 9 Optimal cross-section design of the composite floor system with welded steel sections

In the case when the standard IPE steel sections composed the composite floor structure, the generated superstructure was comprised of:

- 3 different ($m_{fy}$) structural steel grades (S 235, S 275, S 355), $m_{fy} \in M_{fy}$, $M_{fy} = \{1, 2, 3\}$;
- 7 different ($m_{ck}$) concrete strengths (C20/25, C25/30, C30/37, C35/45, C40/50, C45/55, C50/60), $m_{ck} \in M_{ck}$, $M_{ck} = \{1, 2, 3,..., 7\}$;
- 18 different ($s_{IPE}$) standard IPE steel section alternatives (from IPE 80 to IPE 600), $s_{IPE} \in S_{IPE}$, $S_{IPE} = \{1, 2, 3,..., 18\}$;
- 25 different ($s_{mesh}$) discrete alternatives of steel wire meshes for reinforcing the concrete (from R188 to 5xR524), $s_{mesh} \in S_{mesh}$, $S_{mesh} = \{1, 2, 3,..., 25\}$ and
- 27 various ($r_d$) discrete alternatives for rounding up the depth of the concrete slab to a whole cm (from 4 to 30 cm), $r_d \in R_d$, $R_d = \{1, 2, 3,..., 27\}$.

In this case, the number of defined discrete binary variables was $m_{fy} + m_{ck} + s_{IPE} + s_{mesh} + r_d = 3 + 7 + 18 + 25 + 27 = 80$, whilst the superstructure included $m_{fy} \cdot m_{ck} \cdot s_{IPE} \cdot s_{mesh} \cdot r_d = 3 \cdot 7 \cdot 18 \cdot 25 \cdot 27 = 2.5515 \cdot 10^5$ various solutions of discrete variables. The MINLP optimization model COMBOPT of the structure with standard IPE sections was used. The model included the accurate cost objective function, see Eq. (1).

The best result was obtained in the case when the neutral axis lay within the steel web, see the IPE case (c) in Table 4. Whilst the result with continuous parameters of 176.67 € per m$^2$ of the structure was obtained at the 1$^{st}$ NLP, the real result yielded 180.20 € per m$^2$ during the 3$^{rd}$ MINLP iteration (3$^{rd}$ NLP, IPE case (c), Table 4). The optimal solution was also comprised of steel and concrete grades S 235 and C35/45, respectively, standard IPE 600 steel sections and their intermediate distances, depth of the concrete slab 5 cm and the reinforcement R188, see Fig. 10. Note that this solution is more than twice the expense when compared to the solution with welded steel sections. The highest IPE sections - IPE 600 - are actually no longer appropriate for spans of 20 m. Due to too small cross-sectional areas and other characteristics of the sections, the latter were condensed during the optimization process into carrying lower loads. Shorter intermediate distances between the sections were consequently calculated.

When standard HEA steel sections built the composite floor structure, the generated superstructure was similar to the one with IPE sections. Instead of the before-mentioned IPE alternatives, the superstructure was comprised of 24 different ($s_{HEA}$) standard HEA section alternatives (from HEA 100 to HEA 1000), $s_{HEA} \in S_{HEA}$, $S_{HEA} = \{1, 2, 3,..., 24\}$. Whilst the number of defined discrete binary variables was $m_{fy} + m_{ck} + s_{HEA} + s_{mesh} + r_d = 3 + 7 + 24 + 25 + 27 = 86$, the superstructure included $m_{fy} \cdot m_{ck} \cdot s_{HEA} \cdot s_{mesh} \cdot r_d = 3 \cdot 7 \cdot 24 \cdot 25 \cdot 27 = 3.4020 \cdot 10^5$ various solutions. The MINLP optimization model COMBOPT of the composite structure with standard HEA sections was used. The accurate cost objective function is defined.
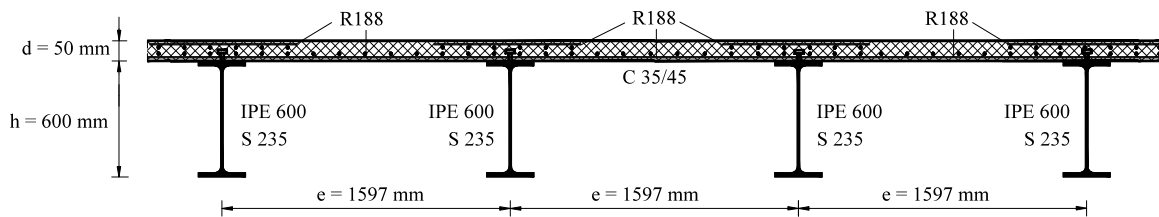


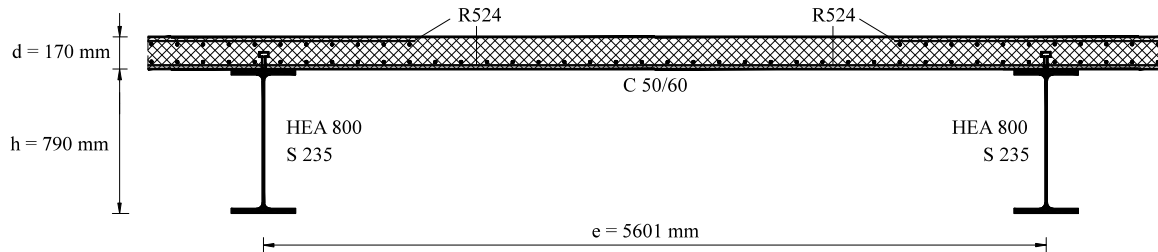Fig. 10 Optimal cross-section design of the composite floor system with standard IPE sections

Fig. 11 Optimal cross-section design of the composite floor system with standard HEA sections

The best result was obtained in the case when the neutral axis lay within the concrete slab, see the HEA case (a) in Table 4. Whilst the result of 128.27 € per m$^2$ of the structure was obtained at the 1$^{st}$ NLP to be the starting point for the discrete optimization, the real result yielded 130.26 € per m$^2$ during the 3$^{rd}$ MINLP iteration (3$^{rd}$ NLP, HEA case (a), Table 4). The optimal solution was also comprised of steel and concrete grades S 235 and C50/60, respectively, standard HEA 800 steel sections and their intermediate distances, depth of the concrete slab 17 cm and the reinforcement R524, see Fig. 11. This solution is 64 per cent more expensive when compared to the solution with welded steel sections, which was found to be the cheapest composite floor structure.

### 5.2 Elastic cross-section resistance

Similarly to the previous calculations, the composite floor structure was also optimized for the case when the elastic cross-section resistances were considered separately for the structure with the welded, IPE and HEA steel sections. The convergence of the algorithm is shown in Table 5. In all three cases, the superstructures and objective functions remained the same as in the calculation of plastic resistance.
The best result for the composite structure with welded I sections was obtained in the case when the neutral axis lay within the steel web. The result yielded 87.04 € per m$^2$ of the structure within the 2$^{nd}$ MINLP iteration (2$^{nd}$ NLP, Welded case (c), Table 5). When standard IPE steel sections composed the composite structure, the best result was gained in the case when the neutral axis was positioned in the steel web. The result reached 179.29 € per m$^2$ of the structure within the 5$^{th}$ MINLP iteration (5$^{th}$ NLP, IPE case (c), Table 5).
Finally, when standard HEA sections built up the composite structure, the best result was calculated in the case when the neutral axis was situated within the concrete slab. The result reached 145.23 € per m$^2$ of the structure within the 2$^{nd}$ MINLP iteration (2$^{nd}$ NLP, HEA case (a), Table 5).
Similarly to the calculations of the composite structure with plastic resistance, the result of the structure with welded steel sections was also found here to be much better that those with IPE and HEA sections, which indicates that standard IPE and HEA sections are inappropriate solutions for a span of 20 m. The results of the composite floor structure with composed welded and HEA sections were in the case of elastic cross-section resistance about 10 per cent worse when compared to the results obtained for the structures with plastic resistance. When IPE steel sections composed the structure, both the results for plastic and elastic resistances were nearly the same. As the solutions of the composite structure based on elastic resistance were in general worse, they are not presented in this paper in detail.

Table 5 Convergence of the Modified OA/ER algorithm for elastic resistance of the composite structure with welded, IPE and HEA sections; results - structure cost [€/m$^2$]

| | Welded | | | IPE | | | HEA | | |
|---|---|---|---|---|---|---|---|---|---|
| | (a) | (b) | (c) | (a) | (b) | (c) | (a) | (b) | (c) |
| Continuous optimization | | | | | | | | | |
| 1. NLP | 89.26 | 88.78 | 86.65 | 220.66 | 217.14 | 174.69 | 135.94 | 133.33 | 135.77 |
| Discrete material, standard and rounded dimension optimization | | | | | | | | | |
| 1. MILP | 88.93 | 89.02 | 86.95 | 225.46 | 221.72 | 177.77 | 133.09 | 133.96 | 139.37 |
| 2. NLP | **98.22** | **88.99** | **87.04** | 225.51[*] | **221.73** | 181.52 | **145.23** | 137.07[*] | **145.37** |
| 2. MILP | 89.07 | 89.63 | 87.10 | 226.11 | 223.09 | 178.13 | 123.67 | 135.26 | 140.44 |
| 3. NLP | 99.28 | 89.71 | 87.15 | **225.99** | 222.73 | 180.20 | 159.87[*] | 139.17[*] | 146.37 |
| 3. MILP | - | - | - | 227.02 | - | 181.25 | 123.83 | 135.45 | - |
| 4. NLP | - | - | - | 226.25 | - | 179.70 | 162.15[*] | 139.02[*] | - |
| 4. MILP | - | - | - | - | - | 182.53 | 123.86 | 135.56 | - |
| 5. NLP | - | - | - | - | - | **179.29** | 161.24[*] | 138.51[*] | - |
| 5. MILP | - | - | - | - | - | 183.37 | 123.94 | 135.69 | - |
| 6. NLP | - | - | - | - | - | 186.50 | 162.13[*] | 148.63 | - |
| 6. MILP | - | - | - | - | - | - | 123.97 | 140.03 | - |
| 7. NLP | - | - | - | - | - | - | 161.11[*] | 150.01 | - |
| - | - | - | - | - | - | - | - | - | - |
| 12. MILP | - | - | - | - | - | - | 124.53 | - | - |
| 13. NLP | - | - | - | - | - | - | 159.33 | - | - |

The neutral axis lies within (a) concrete slab; (b) upper steel flange; (c) steel web
[*]Locally infeasible solution (when a/some constraint(s) is/are not satisfied)

## 6. Conclusions

This paper has presented the cost optimization of a composite floor system. The composite floor system was designed to be connected together from the reinforced concrete slab and steel I sections. The optimization was performed by the mixed-integer non-linear programming (MINLP) approach.

In order to consider various design possibilities, a number of different MINLP optimization models COMBOPT were developed for the optimizations of composite structures with welded, standard HEA and IPE steel sections, with plastic and elastic resistances, at three different positions of the neutral axis (within the concrete slab, the upper steel flange, and the web of steel section) as well as with two different positions of the centre of gravity axis of the transformed (all-steel) section (within the concrete slab and the steel section).

An accurate economic objective function of the self-manufacturing cost was developed, for the structures with welded and standard steel I sections separately. The material, power and labour costs were accounted for within the objective function, subject to the given design, resistance and deflection (in)equality constraints, in order to satisfy the requirements of both the ultimate and serviceability limit states. Eurocode 4 standard was considered for the steel components. The

Modified OA/ER algorithm and the two-phased MINLP optimization were applied.

A numerical example of the optimization of the composite floor system is presented at the end of the paper to enhance the steps and capabilities of the proposed MINLP optimization approach. The developed program tool, particularly different optimization models COMBOPT, enabled us to conduct an accurate study of the design and economic properties of the composite floor system, designed with welded or standard steel I sections, and treated with plastic or elastic cross-section resistances.

## Acknowledgments

## References

Abadie, J. and Carpentier, J. (1969), *Generalization of the Wolfe Reduced Gradient Method to the Case of Nonlinear Constraints*, Optimization (R. Fletcher, Ed.), Academic Press, New York, NY, USA.

Adeli, H. and Kim, H. (2001), "Cost optimization of welded of composite floors using neural dynamics model", *Commun. Numer. Methods Eng.*, **17**(11), 771-787.

Brooke, A., Kendrick, D. and Meeraus A. (1988), *GAMS - A User's Guide*, Scientific Press, Redwood City, CA, USA.

Cheng, L. and Chan, C.M. (2009), "Optimal lateral stiffness design of composite steel and concrete tall frameworks", *Eng. Struct.*, **31**(2), 523-533.

CPLEX (2016), User Notes, ILOG Inc.

Drudd, A.S. (1994), "CONOPT – A large-scale GRG code", *ORSA J. Comput.*, **6**(2), 207-216.

Eurocode 1 (2002), Actions on structures; European Committee for Standardization, Brussels, Belgium.

Eurocode 2 (2004), Design of concrete structures; European Committee for Standardization, Brussels, Belgium.

Eurocode 3 (2005), Design of steel structures; European Committee for Standardization, Brussels, Belgium.

Eurocode 4 (2004), Design of composite steel and concrete structures - Part 1-1: General rules and rules for buildings; European Committee for Standardization, Brussels, Belgium.

Kassapoglou, C. and Dobyns, A.L. (2001), "Simultaneous cost and weight minimization of postbuckled composite panels under combined compression and shear", *Struct. Multidisc. Optim.*, **21**(5), 372-382.

Kaveh, A. and Abadi, A.S.M. (2010), "Cost optimization of a composite floor system using an improved harmony search algorithm", *J. Construct. Steel Res.*, **66**(5), 664-669.

Kaveh, A. and Ahangaran, M. (2012), "Discrete cost optimization of composite floor system using social harmony search model", *Appl. Soft Comput.*, **12**(1), 372-381.

Kaveh, A. and Behnam, A.F. (2012), "Cost optimization of a composite floor system, one-way waffle slab, and concrete slab formwork using a charged system search algorithm", *Scientia Iranica A.*, **19**(3), 410-416.

Kaveh, A. and Ghafari, M.H. (2016), "Optimum design of steel floor system: effect of floor division number, deck thickness and castellated beams", *Struct. Eng. Mech., Int. J.*, **59**(5), 933-950.

Kaveh, A. and Massoudi, M.S. (2012), "Cost optimization of a composite floor system using ant colony system", *Iran. J. Sci. Technol.*, **36**(C2), 139-148.

Klanšek, U. and Kravanja, S. (2006a), "Cost estimation, optimization and competitiveness of different composite floor systems—Part 1: Self-manufacturing cost estimation of composite and steel structures", *J. Construct. Steel Res.*, **62**(5), 434-448.

Klanšek, U. and Kravanja, S. (2006b), "Cost estimation, optimization and competitiveness of different composite floor systems—Part 2: Optimization based competitiveness between the composite I beams, channel-section and hollow-section trusses", *J. Construct. Steel Res.*, **62**(5), 449-462.

Klanšek, U., Šilih, S. and Kravanja, S. (2006), "Cost optimization of composite floor trusses", *Steel Compos. Struct.*, *Int. J.*, **6**(5), 435-457.

Kovacs, G., Groenwold, A.A., Jarmai, K. and Farkas, J. (2004), "Analysis and optimum design of fibre-reinforced composite structures", *Struct Multidisc Optim.*, **28**(2), 170-179.

Kravanja, Z. (2010), "Challenges in sustainable integrated process synthesis and the capabilities of an MINLP process synthesizer MipSyn", *Comput. Chem. Eng.*, **34**(11), 1831-1848.

Kravanja, Z. and Grossmann, I.E. (1994), "New developments and capabilities in PROSYN - An automated topology and parameter process synthesizer", *Comput. Chem. Eng.*, **18**(11-12), 1097-1114.

Kravanja, S. and Šilih, S. (2003), "Optimization based comparison between composite I beams and composite trusses", *J. Construct Steel Res.*, **59**(5), 609-625.

Kravanja, S., Kravanja, Z. and Bedenik, B.S. (1998a), "The MINLP optimization approach to structural synthesis. Part I: A general view on simultaneous topology and parameter optimization", *International J. Numer. Method. Eng.*, **43**(2), 263-292.

Kravanja, S., Kravanja, Z. and Bedenik, B.S. (1998b), "The MINLP optimization approach to structural synthesis. Part II: Simultaneous topology, parameter and standard dimension optimization by the use of the Linked two-phase MINLP strategy", *Int. J. Numer. Methods Eng.*, **43**(2), 293-328.

Kravanja, S., Kravanja, Z. and Bedenik, B.S. (1998c), "The MINLP approach to structural synthesis. Part III: Synthesis of roller and sliding hydraulic steel gate structures", *Int. J. Numer. Methods Eng.*, **43**(2), 329-364.

Kravanja, S., Soršak, A. and Kravanja, Z. (2003), "Efficient multilevel MINLP strategies for solving large combinatorial problems in engineering", *Optimiz. Eng.*, **4**(1), 97-151.

Kravanja, S., Šilih, S. and Kravanja, Z. (2005), "The multilevel MINLP optimization approach to structural synthesis: the simultaneous topology, material, standard and rounded dimension optimization", *Adv. Eng. Software*, **36**(9), 568-583.

Land, A.H. and Doig, A.G. (1960), "An automatic method of solving discrete programming problems", *Econometrica*, **28**(3), 497-520.

Luo, Y., Wang, M.Y., Zhou, M. and Deng, Z. (2012), "Optimal topology design of steel–concrete composite structures under stiffness and strength constraints", *Comput. Struct.*, **112-113**, 433-444.

Omkar, S.N., Khandelwal, R., Santhosh, Yathindra, Narayana, Naik, G. and Gopalakrishnan, S. (2008), "Artificial immune system for multi-objective design optimization of composite structures", *Eng. Applicat. Artif. Intell.*, **21**(8), 1416-1429.

Omkar, S.N., Senthilnath, J., Khandelwal, R., Naik, G.N. and Gopalakrishnan, S. (2011), "Artificial Bee Colony (ABC) for multi-objective design optimization of composite structures", *Appl. Soft Comput.*, **11**(1), 489-499.

Poitras, G., Lefrançois, G. and Cormier, G. (2011), "Optimization of steel floor systems using particle swarm optimization", *J. Construct. Steel Res.*, **67**(8), 1225-1231.

Senouci, A.B. and Al-Ansari, M.S. (2009), "Cost optimization of composite beams using genetic algorithms", *Adv. Eng. Software*, **40**(11), 1112-1118.

Wolfe, P. (1976), *Methods of Nonlinear Program*ming, John Wiley, New York, NY, USA.

*CC*

## Appendix A
## The design plastic moment resistance of a composite I beam floor system

The design plastic moment resistance $M_{pl,Rd,cb}$ is defined for three different design possibilities, i.e., those cases when the plastic neutral axis $x_p$ is situated: within the concrete slab, within the upper flange of the steel section, and within the web of the steel section. Constraint (A1) defines the plastic neutral axis $x_p$ to be situated within the concrete slab, see Fig. A1. $M_{pl,Rd,cb}$ and $x_p$ are in this case determined by Eqs. (A2) and (A3).

$$\frac{A_a \cdot f_y \cdot \gamma_c}{0.85 \cdot f_{ck} \cdot \gamma_a} \leq 2 \cdot b_e \cdot d \tag{A1}$$

$$M_{pl,Rd,cb} = \left[\frac{h}{2} + d - \frac{xp}{2}\right] \cdot \frac{A_a \cdot f_y}{\gamma_a} \tag{A2}$$

where

$$x_p = \frac{A_a \cdot f_y \cdot \gamma_c}{2 \cdot 0.85 \cdot f_{ck} \cdot b_e \cdot \gamma_a} \tag{A3}$$

Eq. (A4) introduces the necessary condition for the plastic neutral axis $x_p$ located within the upper flange of the steel section, see Fig. A2. The design plastic moment resistance $M_{pl,Rd,cb}$ and the vertical distance of the axis $x_p$ from the top edge are then calculated by Eqs. (A5) and (A6), respectively.

$$2 \cdot b_e \cdot d < \frac{A_a \cdot f_y \cdot \gamma_c}{0.85 \cdot f_{ck} \cdot \gamma_a} \leq 2 \cdot b_e \cdot d + 2 \cdot \frac{f_y \cdot \gamma_c}{0.85 \cdot f_{ck} \cdot \gamma_a} \cdot b_f \cdot t_f \tag{A4}$$

$$M_{pl,Rd,cb} = \left[A_a \cdot \left(\frac{h}{2} + \frac{d}{2}\right) - b_f \cdot x_p \cdot (x_p - d)\right] \cdot \frac{f_y}{\gamma_a} \tag{A5}$$

where

$$x_p = d + \frac{A_a}{2 \cdot b_f} - \frac{0.85 \cdot f_{ck} \cdot \gamma_a \cdot b_e \cdot d}{b_f \cdot f_y \cdot \gamma_c} \tag{A6}$$
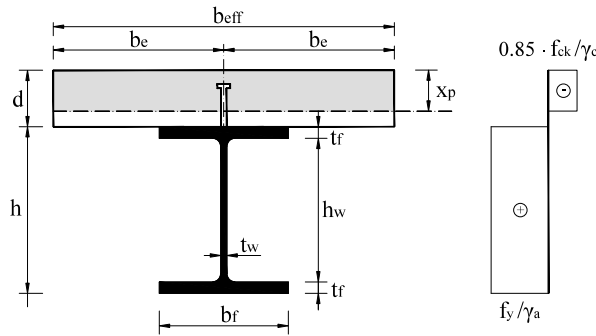


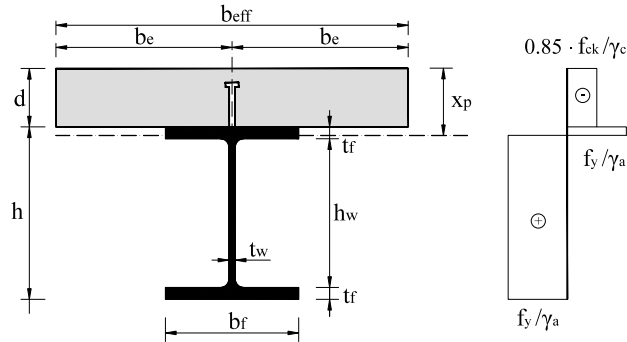Fig. A1 Plastic neutral axis situated within the concrete slab

Fig. A2 Plastic neutral axis situated within the upper flange of the steel section
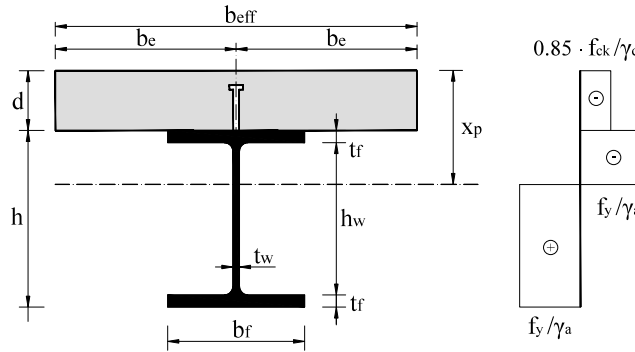


Fig. A3 Plastic neutral axis situated within the web of the steel section

The constraint Eq. (A7) denotes the necessary condition for the plastic neutral axis $x_p$ to be positioned within the web of the steel section, see Fig. A3. $M_{pl,Rd,cb}$ and $x_p$ are in this case defined by Eqs. (A8) and (A9).

$$\frac{f_y \cdot \gamma_c}{0.85 \cdot f_{ck} \cdot \gamma_a} \cdot \left(A_a - 2 \cdot b_f \cdot t_f\right) > 2 \cdot b_e \cdot d \tag{A7}$$

$$M_{pl,Rd,cb} = \left[A_a \cdot \left(\frac{h}{2} + \frac{d}{2}\right) - t_f \cdot b_f \cdot \left(d + t_f\right) - t_w \cdot \left(x_p - t_f - d\right) \cdot \left(x_p + t_f\right)\right] \cdot \frac{f_y}{\gamma_a} \tag{A8}$$

where

$$x_p = d + t_f + \frac{A_a}{2 \cdot t_w} - \frac{0.85 \cdot f_{ck} \cdot \gamma_a \cdot b_e \cdot d}{t_w \cdot f_y \cdot \gamma_c} - \frac{t_f \cdot b_f}{t_w} \tag{A9}$$

## Appendix B
## The design elastic moment resistance of a composite I beam floor system

The design elastic bending moment resistance $M_{el,Rd,cb}$ is proposed as being determined for three different design alternatives, i.e., for three various positions of the elastic neutral axis $x_e$: within the concrete slab, within the upper flange of the steel section and within the steel web. Eqs. (B1)-(B10) introduce the constraints for the elastic neutral axis $x_e$ located within the concrete slab, see Fig. B1. The elastic moment resistance $M_{el,Rd,cb}$ is given by Eq. (B2). Whilst the internal tension forces in steel $N_{t1}$, $N_{t2}$ and $N_{t3}$ are calculated by Eqs. (B3)-(B5), the internal compression force in concrete $N_c$ is defined by Eq. (B6), where $n$ is the modular ratio and $\sigma_a$ is the maximal tension stress in steel beam. The intermediate distances between the internal forces and the neutral axis $a_1$, $a_2$, $a_3$ and $a_4$ are proposed by Eqs. (B7)-(B10).

$$x_e \leq d \tag{B1}$$

$$M_{el,Rd,cb} = N_{t1} \cdot a_1 + N_{t2} \cdot a_2 + N_{t3} \cdot a_3 + N_c \cdot a_4 \tag{B2}$$

where

$$N_{t1} = \frac{\sigma_a}{2} \cdot \left( 1 + \frac{d + h - x_e - t_f}{d + h - x_e} \right) \cdot t_f \cdot b_f \tag{B3}$$

$$N_{t2} = \frac{\sigma_a}{2} \cdot \left( \frac{2 \cdot d + h - 2 \cdot x_e}{d + h - x_e} \right) \cdot (h - 2 \cdot t_f) \cdot t_w \tag{B4}$$

$$N_{t3} = \frac{\sigma_a}{2} \cdot \left( \frac{2 \cdot d + t_f - 2 \cdot x_e}{d + h - x_e} \right) \cdot t_f \cdot b_f \tag{B5}$$

$$N_c = \frac{\sigma_a}{2 \cdot n} \cdot \left( \frac{x_e}{d + h - x_e} \right) \cdot x_e \cdot b_{eff} \tag{B6}$$

$$a_1 = d + h - x_e - \left[ \frac{3 \cdot d + 3 \cdot h - 3 \cdot x_e - 2 \cdot t_f}{2 \cdot d + 2 \cdot h - 2 \cdot x_e - t_f} \cdot \frac{t_f}{3} \right] \tag{B7}$$
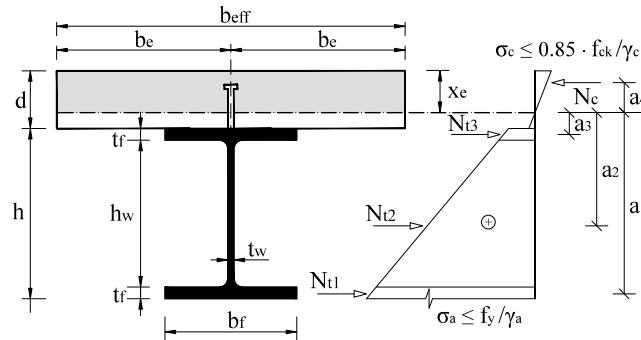


Fig. B1 Elastic neutral axis is situated within the concrete slab
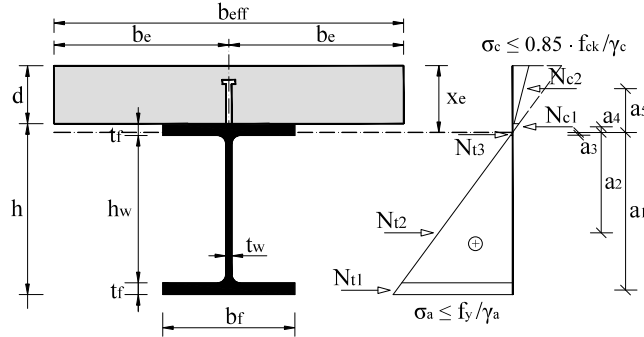
Fig. B2 Elastic neutral axis situated within the upper flange of the steel section

$$a_2 = d + h - x_e - t_f - \left[ \frac{3 \cdot d + h + t_f - 3 \cdot x_e}{2 \cdot d + h - 2 \cdot x_e} \cdot \frac{(h - 2 \cdot t_f)}{3} \right]$$ (B8)

$$a_3 = d + t_f - x_e - \left[ \frac{3 \cdot d + t_f - 3 \cdot x_e}{2 \cdot d + t_f - 2 \cdot x_e} \cdot \frac{t_f}{3} \right]$$ (B9)

$$a_4 = 2/3 \cdot x_e$$ (B10)

Eqs. (B11)-(B22) denote the constraints for the elastic neutral axis $x_e$ positioned within the upper flange of the steel section, see Fig. B2. The elastic bending moment resistance is determined by Eq. (B12). Eqs. (B13)-(B15) represent the internal tension forces in steel $N_{t1}$, $N_{t2}$ and $N_{t3}$, whilst Eqs. (B16)-(B17) stand for the internal compression forces within concrete $N_{c1}$ and $N_{c2}$. The distances between the forces and the neutral axis $a_1$, $a_2$, $a_3$, $a_4$ and $a_5$ are proposed by Eq. (B18)-(B22).

$$d \le x_e \le \left( d + t_f \right)$$ (B11)

$$M_{el,Rd,cb} = N_{t1} \cdot a_1 + N_{t2} \cdot a_2 + N_{t3} \cdot a_3 + N_{c1} \cdot a_4 + N_{c2} \cdot a_5$$ (B12)

where

$$N_{t1} = \frac{\sigma_a}{2} \cdot \left( 1 + \frac{d + h - x_e - t_f}{d + h - x_e} \right) \cdot t_f \cdot b_f$$ (B13)

$$N_{t2} = \frac{\sigma_a}{2} \cdot \left( \frac{2 \cdot d + h - 2 \cdot x_e}{d + h - x_e} \right) \cdot \left( h - 2 \cdot t_f \right) \cdot t_w$$ (B14)

$$N_{t3} = \frac{\sigma_a}{2} \cdot \left( \frac{d + t_f - x_e}{d + h - x_e} \right) \cdot \left( d + t_f - x_e \right) \cdot b_f$$ (B15)

$$N_{c1} = \frac{\sigma_a}{2} \cdot \left( \frac{x_e - d}{d + h - x_e} \right) \cdot (x_e - d) \cdot b_f$$ (B16)

$$N_{c2} = \frac{\sigma_a}{2 \cdot n} \cdot \left(\frac{2 \cdot x_e - d}{d + h - x_e}\right) \cdot d \cdot b_{eff} \tag{B17}$$

$$a_1 = d + h - x_e - \left[\frac{3 \cdot d + 3 \cdot h - 3 \cdot x_e - 2 \cdot t_f}{2 \cdot d + 2 \cdot h - 2 \cdot x_e - t_f} \cdot \frac{t_f}{3}\right] \tag{B18}$$

$$a_2 = d + h - x_e - t_f - \left[\frac{3 \cdot d + h + t_f - 3 \cdot x_e}{2 \cdot d + h - 2 \cdot x_e} \cdot \frac{(h - 2 \cdot t_f)}{3}\right] \tag{B19}$$

$$a_3 = 2/3 \cdot \left(d + t_f - x_e\right) \tag{B20}$$

$$a_4 = 2/3 \cdot (x_e - d) \tag{B21}$$

$$a_5 = x_e - \left[\frac{3 \cdot x_e - 2 \cdot d}{2 \cdot x_e - d} \cdot \frac{d}{3}\right] \tag{B22}$$

Eqs. (B23)-(B34) stand for the constraints for the elastic neutral axis $x_e$ lying within the web of the steel section, see Fig. B3. The elastic moment resistance $M_{el,Rd,cb}$ is proposed by Eq. (B24). Whilst the internal tension forces in steel $N_{t1}$ and $N_{t2}$ are calculated by Eqs. (B25) and (B26), the internal compression forces in concrete $N_{c1}$, $N_{c2}$ and $N_{c3}$ are defined by Eqs. (B27)-(B29). The intermediate distances between the forces and the neutral axis $a_1$, $a_2$, $a_3$, $a_4$ and $a_5$ are determined by Eqs. (B30)-(B34).

$$x_e \geq (d + t_f) \tag{B23}$$

$$M_{el,Rd,cb} = N_{t1} \cdot a_1 + N_{t2} \cdot a_2 + N_{c1} \cdot a_3 + N_{c2} \cdot a_4 + N_{c3} \cdot a_5 \tag{B24}$$

where

$$N_{t1} = \frac{\sigma_a}{2} \cdot \left(1 + \frac{d + h - x_e - t_f}{d + h - x_e}\right) \cdot t_f \cdot b_f \tag{B25}$$

$$N_{t2} = \frac{\sigma_a}{2} \cdot \left(\frac{d + h - x_e - t_f}{d + h - x_e}\right) \cdot \left(d + h - x_e - t_f\right) \cdot t_w \tag{B26}$$
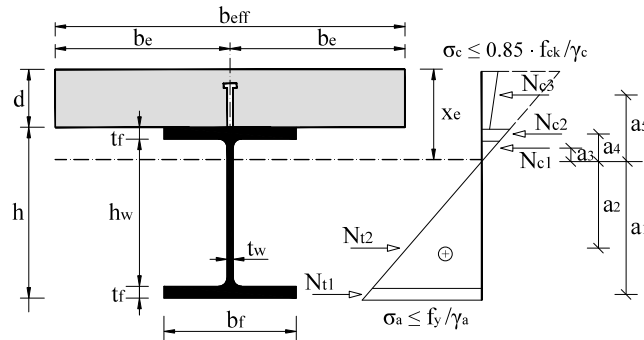


Fig. 3 Elastic neutral axis situated within the web of the steel section

$$N_{c1} = \frac{\sigma_a}{2} \cdot \left( \frac{x_e - d - t_f}{d + h - x_e} \right) \cdot \left( x_e - d - t_f \right) \cdot t_w \tag{B27}$$

$$N_{c2} = \frac{\sigma_a}{2} \cdot \left( \frac{2 \cdot x_e - 2 \cdot d - t_f}{d + h - x_e} \right) \cdot t_f \cdot b_f \tag{B28}$$

$$N_{c3} = \frac{\sigma_a}{2 \cdot n} \cdot \left( \frac{2 \cdot x_e - d}{d + h - x_e} \right) \cdot d \cdot b_{eff} \tag{B29}$$

$$a_1 = d + h - x_e - \left[ \frac{3 \cdot d + 3 \cdot h - 3 \cdot x_e - 2 \cdot t_f}{2 \cdot d + 2 \cdot h - 2 \cdot x_e - t_f} \cdot \frac{t_f}{3} \right] \tag{B30}$$

$$a_2 = 2/3 \cdot \left( d + h - x_e - t_f \right) \tag{B31}$$

$$a_3 = 2/3 \cdot \left( x_e - d - t_f \right) \tag{B32}$$

$$a_4 = x_e - d - \left[ \frac{3 \cdot x_e - 3 \cdot d - 2 \cdot t_f}{2 \cdot x_e - 2 \cdot d - t_f} \cdot \frac{t_f}{3} \right] \tag{B33}$$

$$a_5 = x_e - \left[ \frac{3 \cdot x_e - 2 \cdot d}{2 \cdot x_e - d} \cdot \frac{d}{3} \right] \tag{B34}$$